http://dx.doi.org/10.15576/GLL/2015.2.33

GLL

Geomatics, Landmanagement and Landscape No. 2 • 2015, 33–44

CORRECTIONS TO SEA LEVEL ANOMALIES DATA DUE TO GEOCENTER MOTION

Wiesław Kosek, Agnieszka Wnęk, Maria Zbylut-Górska

Summary

The objective of this paper is computation of the corrections to sea level anomaly data due to center of Earth mass variations. The geocenter motion model was computed from the center of mass coordinates data determined from observations of space geodetic techniques such as Satellite Laser Ranging (SLR), Global Navigation Satellite System (GNSS) and Doppler Orbitography and Radiopositionig Integrated on Satellite (DORIS). In order to compute the geocenter motion model the center of mass coordinates data were filtered using wavelet based semblance filtering which allows computing a common signal in two time series. Based on determined geocenter motion model a correction to sea level anomalies (SLA) data due to geocenter motion was determined. This kind of correction to sea level anomaly data is of the order of few millimetres and should be applied to altimetric measurements to refer them to the International Terrestrial Reference Frame (ITRF) Origin considered as the center of figure.

Keywords

geocenter • sea level anomalies • wavelet based semblance filtering

1. Introduction

The center of mass of the Earth (CM) is the centre of the whole Earth including its fluid layers such as atmosphere, oceans and continental waters. The CM is distinguished from the center of figure (CF) which is recognized as the origin of the International Terrestrial Reference Frame (ITRF). Due to mass redistributions in the Earth's fluid layers the CM is instantaneous and its variations with respect to the CF are defined as geocenter motion [Petit and Luzum 2010]. Position of the geocenter has a significant influence on altimetric measurements since altimetric satellites orbit around the instantaneous CM, while its orbits are determined in the ITRF with a fixed origin (currently ITRF2008).

Actually, geocenter time series are determined based on observations from all satellites geodesy techniques such as Satellite Laser Ranging (SLR), Global Navigation Satellite System (GNSS) and Doppler Orbitography and Radiopositionig Integrated on Satellite (DORIS). Previous studies [Kosek et al. 2014] indicated that the DORIS,

GNSS and SLR geocenter time series show some agreement thus they were filtered using wavelet based semblance filtering. This kind of filtering enables computation a common signal in two time series, thus for this purpose the geocenter time series from different satellites techniques were grouped in the following pairs: GNSS-DORIS, SLR-GNSS, SLR-DORIS. The three common signals in geocenter time series were then used to construct a stochastic model of the geocenter motion. The obtained model was subsequently used to compute time corrections to the global sea level anomaly (SLA) data due to geocenter variations.

2. Data

In the analyses the weekly geocenter time series from DORIS, GNSS and SLR were used.

SLR geocenter data named GEOC94–13.GCC–1 were computed by Astronomical Institute of the University of Bern and come from years 1994 – 2014 [Sosnica et al. 2011, 2013]. The SLR geocenter time series is expressed in the SLR terrestrial reference frame (TRF) called SLRF2008 which is linked to the ITRF2008.

GNSS geocenter time series are combined solutions 5–4_igs.sum and are delivered by International GNSS Service (IGS) in 1994–2014 [IGS, 2014]. These geocenter time series are determined in IGS reference frame IGb08 which is also linked to the ITRF2008.

DORIS geocenter data set ign11wd01.geoc is available at Crustal Dynamics Data Information System (CDDIS) from 1994 to 2014 [Willis et al. 2005a, b, 2012] and is expressed in the ITRF2008.

3. Wavelet based semblance filtering

In order to filter the geocenter time series obtained from observations of three independent space techniques the wavelet semblance filtering [Cooper 2009] was applied. This type of filtering of the geocenter time series has been widely described by Kosek et al. [2014].

The wavelet semblance filtering allows computing a common signal in two time series. In order to determine such signal, two time series were transformed into time-frequency domain using the discrete wavelet transform (DWT) with Shannon wavelet functions. The computed wavelet transform coefficients of both time series were then used to estimate the semblance function. Assuming a fixed semblance threshold, zero values were assigned to wavelet transform coefficients of analysed time series, for which the semblance was below this threshold. Next, the inverse DWT was used to determine the common signals in three pairs SLR-DORIS, SLR-GNSS and GNSS-DORIS of the considered time series by summing 6 filtered lowest frequency components. Afterwards, to compute the common signals from the two time series of three pairs of satellites techniques the weighted averages were computed. The weights of the corresponding technique pairs were assumed as inversely proportional to the variances

of the corresponding filtered geocenter signals. Figures 1, 2 and 3 present the common signals in SLR-DORIS, SLR-GNSS and GNSS-DORIS pairs, respectively.

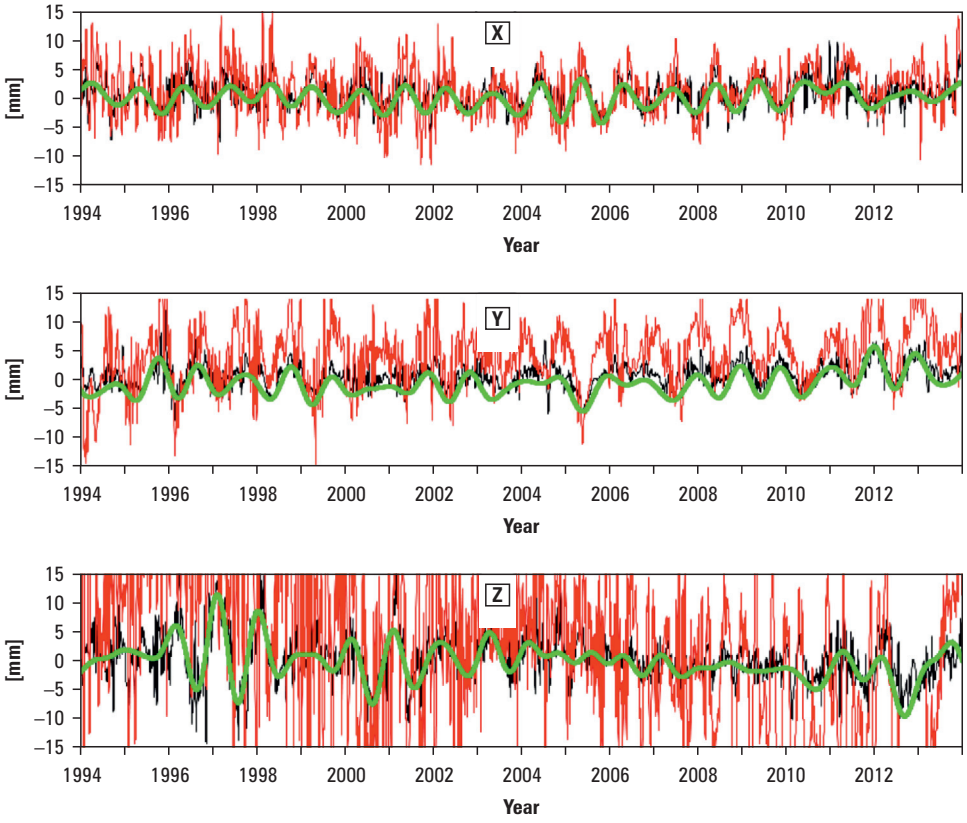

Source: authors' study

Fig. 1. The common oscillations computed by the wavelet semblance filtering (threshold equal 0.90) between the SLR (black) and DORIS (red) geocenter time series. Smoothed bright green lines correspond to the weighted average of common signals reconstructed using the 6 lowest frequency components

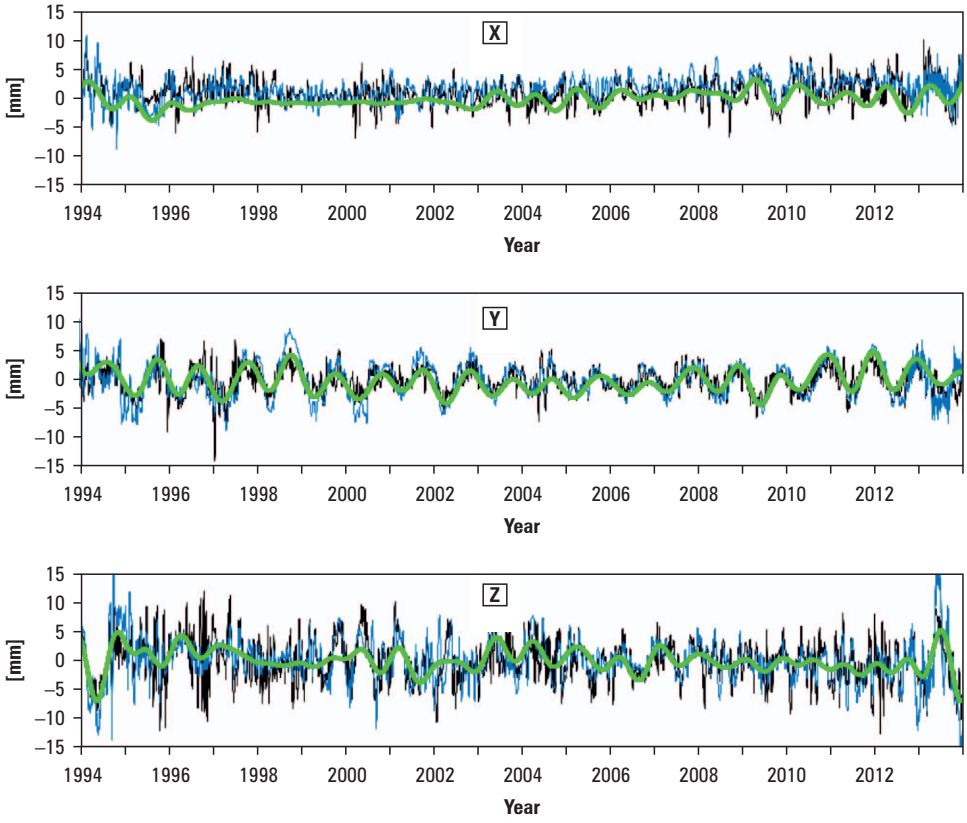

Source: authors' study

Fig. 2. The common oscillations computed by the wavelet semblance filtering (threshold equal 0.90) between the SLR (black) and GNSS (blue) geocenter time series. Smoothed bright green lines correspond to the weighted average of common signals reconstructed using the 6 lowest frequency components

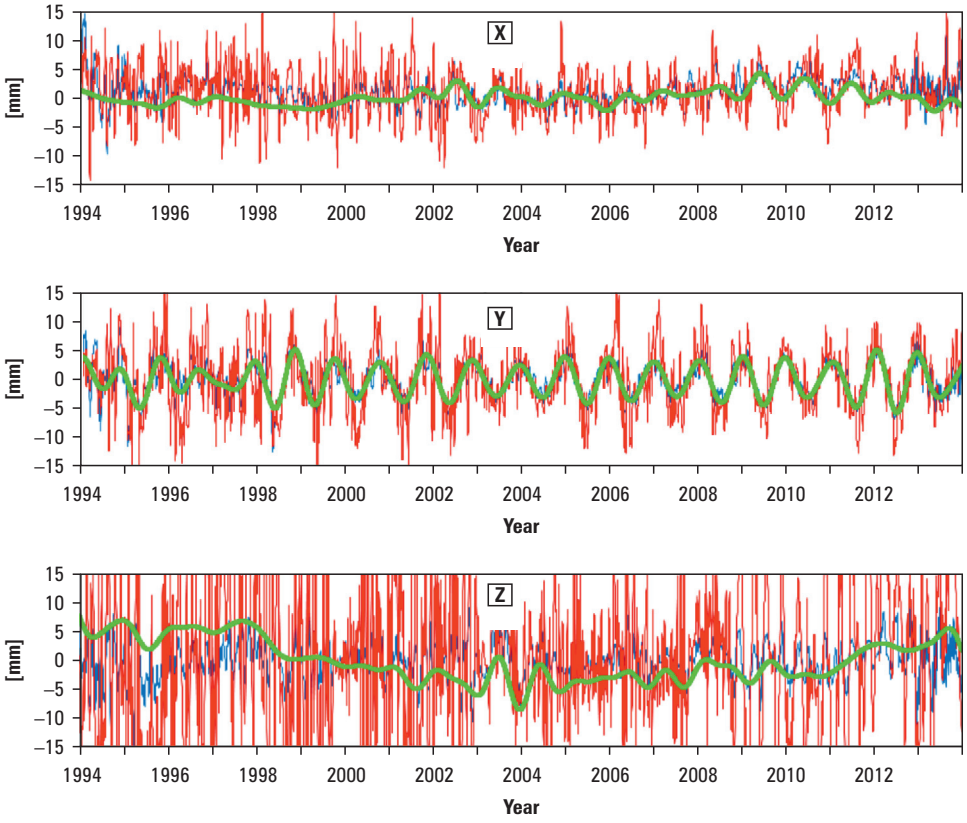

Source: authors' study

Fig. 3. The common oscillations computed by the wavelet semblance filtering (threshold equal 0.90) between the GNSS (blue) and DORIS (red) geocenter time series. Smoothed bright green lines correspond to the weighted average of common signals reconstructed using the 6 lowest frequency components

The three common signals in geocenter time series were then used to construct a stochastic model representing geocenter motion determined from observations of three independent techniques. Finally, the geocenter motion model $[x_g(t), y_g(t), z_g(t)]$ was computed using the weighted average of three common signals. The weights of each technique pair were assumed as inversely proportional to the variance of the corresponding common signals. The final geocenter motion stochastic model is shown in Figure 4.

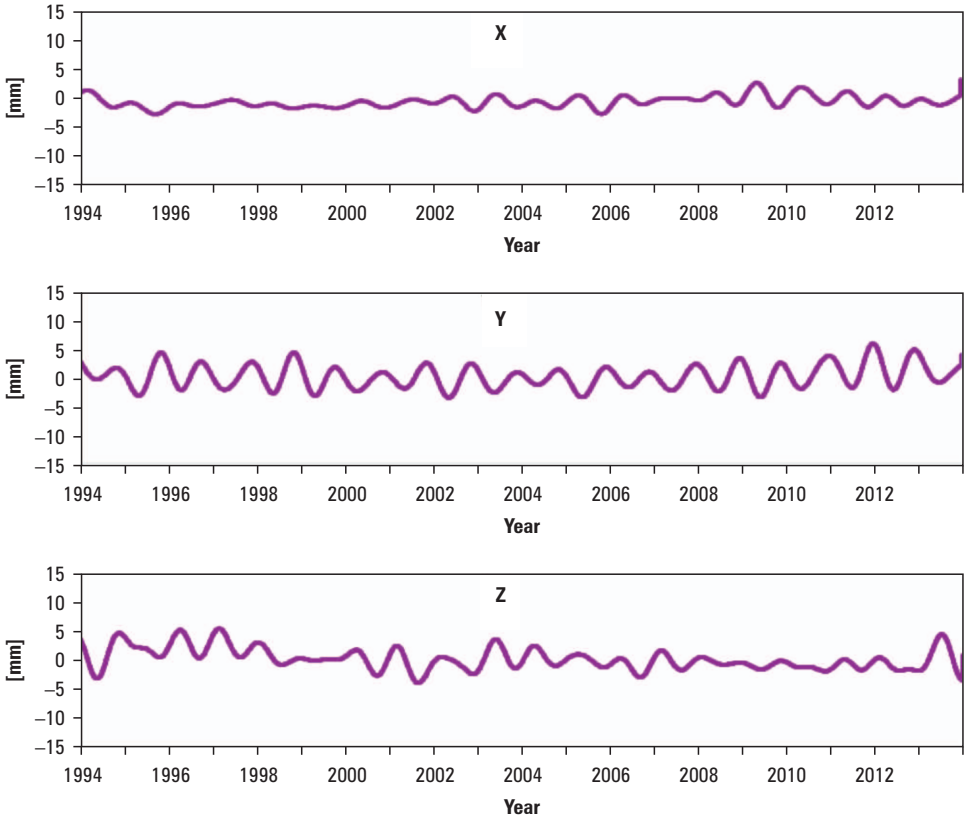

Source: authors' study

Fig. 4. The stochastic geocenter motion model determined as weighted average of bright green lines (shown in Figures 1, 2 and 3) corresponding to pairs of different techniques

4. Correction to SLA data due to geocenter motion

The geocenter motion stochastic model was then used to compute time corrections to the global sea level anomaly data.

First, each ocean grid with coordinates φ, λ was transformed from ellipsoidal to Cartesian coordinates assuming the height above the ellipsoid equal to zero ($h = 0$) [Lamparski 2001]:

$$\begin{pmatrix} X \\ Y \\ Z \end{pmatrix} = \begin{pmatrix} (\bar{N} + h)\cos\varphi \cos\lambda \\ (\bar{N} + h)\cos\varphi \sin\lambda \\ ((1 - e^2)\bar{N} + h)\sin\varphi \end{pmatrix} \tag{1}$$

where:

$$e^2 = \frac{a^2 - b^2}{a^2}, \qquad \bar{N} = \frac{a}{\sqrt{1 - e^2 \sin^2\varphi}} \tag{2}$$

Afterwards, the stochastic geocenter motion model $[x_g(t), y_g(t), z_g(t)]$ was added to the Cartesian coordinates of each ocean grid:

$$\begin{pmatrix} X(t) \\ Y(t) \\ Z(t) \end{pmatrix} = \begin{pmatrix} X + x_g(t) \\ Y + y_g(t) \\ Z + z_g(t) \end{pmatrix} \tag{3}$$

The Cartesian coordinates corrected for geocenter motion model were transformed back to ellipsoidal coordinates using the following formulae [Lamparski 2001]:

$$\lambda = \arctan\frac{Y(t)}{X(t)}, \qquad \varphi = \arctan\frac{Z(t) + (e')^2 b\sin^3\Theta}{p'(t) - e^2 a\cos^3\Theta}$$

$$p'(t) = \sqrt{X(t)^2 + Y(t)^2}, \qquad \Theta = \arctan\frac{Z(t)\cdot a}{p'(t)\cdot b}, \qquad (e')^2 = \frac{a^2 - b^2}{b^2} \tag{4}$$

$$h_{\phi,\lambda}(t) = \frac{p'(t)}{\cos\varphi} - \bar{N}$$

The Cartesian coordinates corrected for geocenter motion model can be also transformed back to ellipsoidal coordinates using the following recursive formulae [Osada 2009]:

$$\begin{aligned}
\tan\varphi_o &= \frac{Z(t)}{X(t)\cos\lambda + Y(t)\sin\lambda} & \bar{N}_o &= \frac{a}{\sqrt{1 - e^2\sin^2\varphi_o}} \\
\tan\varphi_1 &= \frac{Z(t) + \bar{N}_o e^2\sin\varphi_o}{X(t)\cos\lambda + Y(t)\sin\lambda} & \bar{N}_1 &= \frac{a}{\sqrt{1 - e^2\sin^2\varphi_1}} \\
\tan\varphi_2 &= \frac{Z(t) + \bar{N}_1 e^2\sin\varphi_1}{X(t)\cos\lambda + Y(t)\sin\lambda} & \bar{N}_2 &= \frac{a}{\sqrt{1 - e^2\sin^2\varphi_2}} \\
&\vdots & &\vdots \\
\tan\varphi_k &= \frac{Z(t) + \bar{N}_{k-1} e^2\sin\varphi_{k-1}}{X(t)\cos\lambda + Y(t)\sin\lambda} & \bar{N}_k &= \frac{a}{\sqrt{1 - e^2\sin^2\varphi_k}}
\end{aligned} \tag{5}$$

This convergence is fast since $h << \bar{N}$ [Seeber 2003] and after computing precision of $\bar{N}_k$ is less than 1 mm then:

$$h_{\varphi,\lambda}(t) = \frac{\sqrt{X(t)^2 + Y(t)^2}}{\cos\varphi_k} - \bar{N}_k \qquad \text{or} \qquad h_{\varphi,\lambda}(t) = \frac{Z(t)}{\sin\varphi_k} - (1 - e^2)\bar{N}_k \tag{6}$$

Both methods of computing height above the ellipsoid give the same results.

Obtained during the transformation height above the ellipsoid *h(t)* is time correction to the SLA data due to geocenter motion.

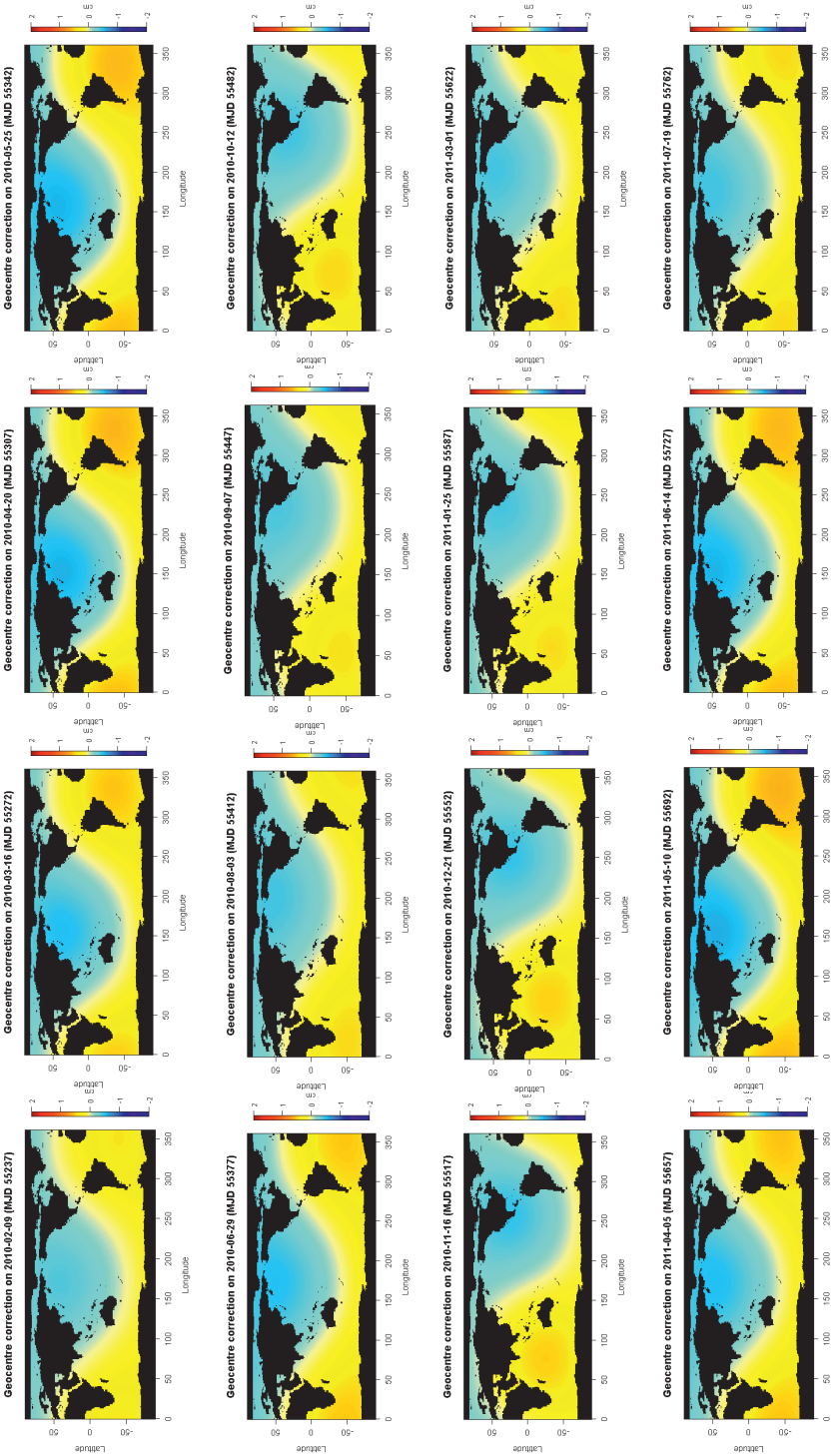

Source: authors' study

Fig. 5. The correction at 35 days sampling interval due to geocenter motion model for period from February 2010 to November 2013

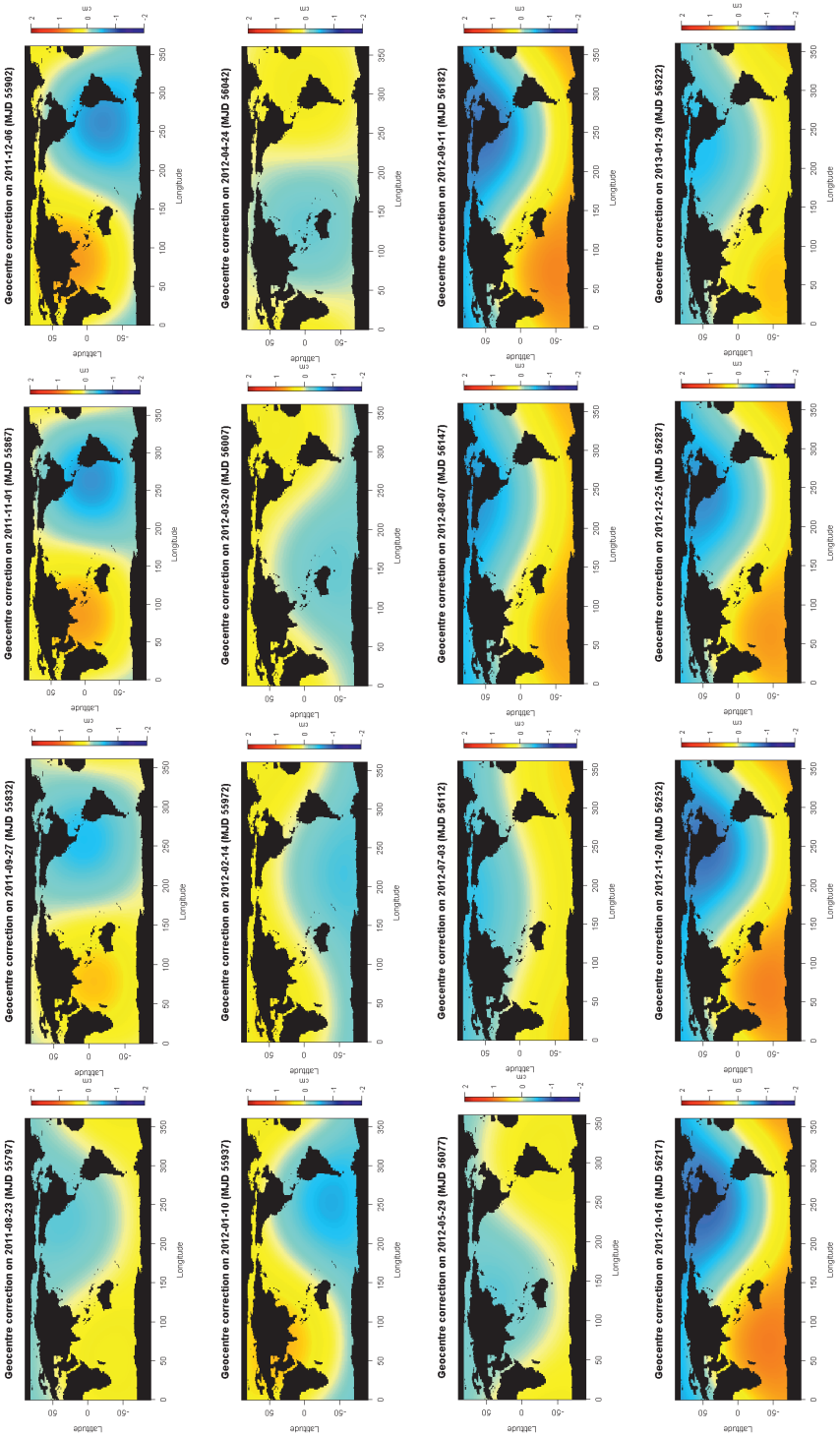
Geocentre correction on 2011-12-06 (MJD 55902)
Geocentre correction on 2012-04-24 (MJD 56042)
Geocentre correction on 2012-09-11 (MJD 56182)
Geocentre correction on 2013-01-29 (MJD 56322)
Geocentre correction on 2011-11-01 (MJD 55867)
Geocentre correction on 2012-03-20 (MJD 56007)
Geocentre correction on 2012-08-07 (MJD 56147)
Geocentre correction on 2012-12-25 (MJD 56287)
Geocentre correction on 2011-09-27 (MJD 55832)
Geocentre correction on 2012-02-14 (MJD 55972)
Geocentre correction on 2012-07-03 (MJD 56112)
Geocentre correction on 2012-11-20 (MJD 56252)
Geocentre correction on 2011-08-23 (MJD 55797)
Geocentre correction on 2012-01-10 (MJD 55937)
Geocentre correction on 2012-05-29 (MJD 56077)
Geocentre correction on 2012-10-16 (MJD 56217)
Latitude
Longitude
cm

Fig. 5. cont.

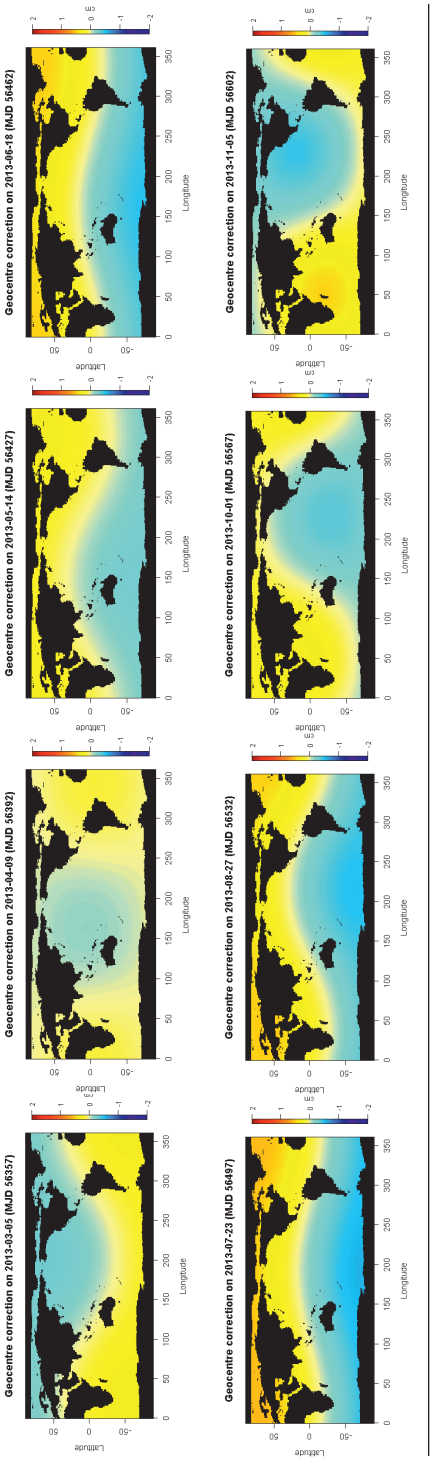
Geocentre correction on 2013-03-05 (MJD 56357)
Geocentre correction on 2013-04-09 (MJD 56392)
Geocentre correction on 2013-05-14 (MJD 56427)
Geocentre correction on 2013-06-18 (MJD 56462)
Geocentre correction on 2013-07-23 (MJD 56497)
Geocentre correction on 2013-08-27 (MJD 56532)
Geocentre correction on 2013-10-01 (MJD 56567)
Geocentre correction on 2013-11-05 (MJD 56602)
Latitude
Longitude
cm

Fig. 5. cont.

Figure 5 shows the maps of the time correction to the SLA data due to geocenter motion with the 35 days sampling intervals from February 2010 to November 2013. This correction was determined based on geocenter variations time series thus it is at the millimetre level.

5. Conclusion

The time series of geocenter motion are actually determined from observations of all satellite geodesy techniques. For this reason it becomes important to propose a one general signal which will be represent geocenter motion taking into account the signals from all three satellites techniques.

The wavelet based semblance filtering enables to compute common oscillations in two time series. Therefore this kind of filtering enables designate common oscillations, which then can be used to determine the stochastic model of geocenter motion. The geocenter motion model can be applied as various type of correction to the geophysical appointments which depend on position of the CM.

The SLA data are taken into account many corrections, for example due to pole coordinates variations, but not include the correction resulting from geocenter motions. Thus, the correction to SLA data due to geocenter motions was purposed because the geocenter variations cause the systematic errors in the sea level anomalies data.

Acknowledgements

This project was financed from the funds of the National Science Centre (Poland) allocated on the basis of the decision number DEC–2013/09/N/ST10/00664.

The research of W. Kosek was supported by the Polish Ministry of Science and Education, project number UMO–2012/05/B/ST10/02132 under the leadership of Prof. A. Brzeziński.

References

Cooper G.R.J. 2009. Wavelet based semblance filtering. Comput. Geosci., 35, 1988–1991.

IGS 2014. ftp://igs-rf.ign.fr/pub/sum/.

Kosek W., Wnęk A., Zbylut-Górska M., Popiński W. 2014. Wavelet analysis of the Earth center of mass time series determined by satellite techniques. J. Geodyn., 80, 58–65.

Lamparski J. 2001. Navstar GPS od teorii do praktyki. Wyd. Uniwersytetu Warmińsko-Mazurskiego, Olsztyn.

Osada E. 2009. Państwowy system odniesień przestrzennych i mapy, Wyd. Dolnośląska Szkoła Wyższa, Wrocław.

Petit G., Luzum B. (eds) 2010. IERS Conventions. IERS Technical Note No. 36, Observatoire de Paris, Paris.

Sosnica K., Thaller D., Dach R., Jäggi A., Beutler G. 2013. Impact of loading displacements on SLR-derived parameters and on the consistency between GNSS and SLR results. J. Geod., 87, 8, 751–769.

Sosnica K., Thaller D., Jäggi A., Dach R., Beutler G. 2011. Reprocessing 17 years of observations to LAGEOS–1 and –2 satellites. GeodätischeWoche2011. Nürnberg, Germany, September 26–29.

Seeber G. 2003. Satellite Geodesy: foundations, methods, and applications / Günther Seeber. 2nd completely rev. and extended ed., Walter de Gruyter, Berlin.

Willis P., Bar-Sever Y.E., Tavernier G. 2005a. DORIS as a potential part of a Global Geodetic Observing System. J. Geodyn., 40, 4–5, 494–501.

Willis P., Boucher C., Fagard H., Altamimi Z. 2005b. Applications geodesiques du systeme DORIS a l'InstitutGeographique National, Geodetic applications of the DORIS system at the French Institute Geographique National, C.R. Geoscience, 337, 7, 653–662.

Willis P., Gobinddass M.L., Garayt B., Fagard H. 2012. Recent improvements in DORIS data processing in view of ITRF2008, the ignwd08 solution, IAG Symposia Series, 136, 43–49.

Prof. dr hab. inż. Wiesław Kosek
Uniwersytet Rolniczy w Krakowie
Katedra Geodezji
30-149 Kraków, ul. Balicka 253a
e-mail: kosek@cbk.waw.pl

Dr inż. Agnieszka Wnęk
Uniwersytet Rolniczy w Krakowie
Katedra Geodezji
30-149 Kraków, ul. Balicka 253a
e-mail: agwnek@ur.krakow.pl

Dr inż. Maria Zbylut-Górska
Uniwersytet Rolniczy w Krakowie
Katedra Geodezji
30-149 Kraków, ul. Balicka 253a
e-mail: mzbylut-gorska@ur.krakow.pl